International Journal of Nanoelectronics and Materials
IJNeaM
ISSN 1985-5761 | E-ISSN 2232-1535

# 2-Axis controlled spray pyrolysis deposition device for Dye-sensitized Solar Cell (DSSC)

Siti Nurhaziqah Abd Majid [a], Muhammad Fikri Bakrin [a], Mohd Khairul Ahmad [a], Faridah Abu Bakar [b], Nik Aziz Nik Ali [c], Diani Galih Saputri [a], Noor Kamalia Abd Hamed [a], Shazleen Ahmad Ramli [a], Mohamad Hafiz Mamat [d], Masaru Shimomura [e], Suriani Abu Bakar [f], Mohd Azwadi Omar [a], Mohd Yazid Ahmad [g], and Jais Lias [h]*

[a]*Microelectronic and Nanotechnology – Shamsuddin Research Centre (MiNT-SRC), 86400 Batu Pahat, Johor, MALAYSIA*
[b]*Faculty of Applied Science and Technology, Universiti Tun Hussein Onn Malaysia, Pagoh Education Hub, 84600 Muar, Johor, MALAYSIA*
[c]*Faculty of Fisheries and Food Science, Universiti Malaysia Terengganu, 21030 Kuala Terengganu, Terengganu, MALAYSIA*
[d]*NANO-ElecTronic Centre (NET), School of Electrical Engineering, College of Engineering, Universiti Teknologi MARA, 40450, Shah Alam, Selangor, MALAYSIA*
[e]*Department of Engineering, Graduate School of Integrated Science and Technology, Shizuoka University, 432-8011, JAPAN*
[f]*Nanotechnology Research Centre, Faculty of Science and Mathematics, Universiti Pendidikan Sultan Idris (UPSI), Tanjung Malim 35900, Perak, MALAYSIA*
[g]*Nanorian Technologies Sdn Bhd, Jln Kajang Perdana 3/2, Taman Kajang Perdana, 43000 Kajang, Selangor, MALAYSIA*
[h]*Faculty of Electrical and Electronic Engineering, Universiti Tun Hussein Onn Malaysia, 86400 Batu Pahat, Johor, MALAYSIA*
** Corresponding author. Tel.: +607-4537000; e-mail: jaisl@uthm.edu.my*

Received 18 January 2024, Revised 3 July 2024, Accepted 7 July 2024

**ABSTRACT**

Dye-sensitized solar cells (DSSCs) are a promising alternative to traditional silicon-based photovoltaic systems due to their efficient light-to-electricity conversion. A critical component of DSSCs is titanium dioxide ($TiO_2$), responsible for converting light into electrical energy. Spray pyrolysis was one of the methods for fabricating $TiO_2$ thin films. However, there are several drawbacks, such as challenges in particle size control, maintaining homogeneity of the thin film, and scalability issues during the deposition process. Modifications to the manufacturing process are necessary to achieve optimal performance in DSSCs, particularly with the thickness of the cell. This work focuses on the 2-axis spray pyrolysis process, a cost-effective way to create thin and thick films. In particular, it focuses on $TiO_2$ thin films utilized as working electrodes in DSSC applications. The method was performed at different motor speeds, namely MS80, MS100, and MS120. The X-ray diffraction (XRD) spectrum showed that the dominance of the anatase phase appeared in an MS100. The UV-Vis results depict that the band gap value is 3.02 eV. The surface profiler analysis indicates that sample MS100 has an optimal thickness of 15.17 µm. The DSSC achieved 9.4% efficiency with sample MS100. This finding demonstrates that using 2-axis controlled spray pyrolysis deposition improves DSSC performance with an optimal motor speed.

**Keywords:** *Dye-sensitized solar cell, Titanium oxide, Spray pyrolysis, 2-axis device*

## 1. INTRODUCTION

Solar power offers a pure, sustainable, and less expensive energy source for people while also serving as a significant energy source for other energy sources, such as wind energy, water, bioenergy, and fossil fuel [1-4]. Solar cells are categorized based on their material composition. These include organic dye solar cells, dye-sensitized, non-crystal, multiple crystals, and single-crystal silicon solar cells [5-7].

Since DSSC use the same principles as photosynthesis in plants and can be produced cheaply, they are anticipated to be among the next generation of solar cells [6, 8-10]. A DSSC has four essential components: a working electrode, a dye, an electrolyte, and a counter electrode [11-13]. Typically, the working electrode used in DSSC is made of titanium dioxide $TiO_2$ material [14-16]. To improve DSSC performance, it is crucial to consider several properties of $TiO_2$ as a working electrode [17]. Some notable characteristics include a large surface area, a nanocrystalline structure, a wide band gap, and others.

Depositing $TiO_2$ onto the Fluorine-doped Tin Oxide (FTO) substrate determines its properties [18]. Deposition of $TiO_2$ on the FTO substrate using many existing methods is often expensive and inefficient [19]. The method used to fabricate $TiO_2$, such as sol-gel, hydrothermal, sputtering, chemical vapour deposition (CVD), electrodeposition, screen printing, or spray pyrolysis, can affect its crystalline structure, surface area, and other characteristics [20]. Out of these methods, spray pyrolysis is usually considered the most optimal.

Spray pyrolysis is being continuously improved to increase the quality of solar cells [21]. Spray pyrolysis techniques are now used in the following applications: standard pyrolysis

via spray deposition, pyrolysis in thin-film deposition spray, jet nebulizer spray pyrolysis (JNSP), flame spray pyrolysis (FSP), jet ultrasonic spray pyrolysis (JUSP), laser pyrolysis (LP), and electrospray pyrolysis (EP) [22]. This manufacturing method offers various benefits, such as the easy process of adding certain substances into the spray composition for doping the films. The process takes place in air ambient, which means that there is no need for vacuum conditions. Additionally, it operates at moderate temperatures, resulting in a simple and compact fabrication process [23].

This process involves several processes, including producing small spray droplets from the precursor solution, solvent evaporation, solute reduction, chemical reaction of the solute, spray droplet breakdown, and the sintering of thin films [24]. There are several drawbacks associated with this method. For instance, it has limited thickness control which results in variations in film thickness [15]. Additionally, spray uniformity is also a concern, as it can lead to non-uniform film thickness. Moreover, this method has a low deposition rate compared to some other methods, which makes it less efficient for large-scale production. There is limited study on 2-Axis Controlled Spray Pyrolysis Deposition Devices for DSSC like Figure 1. This study can lead to optimizing $TiO_2$ deposition on FTO substrate to improve DSSC efficiency.

## 2. METHODOLOGY

This section discusses the fabrication process of $TiO_2$ thin films, including the chemicals used and the 2-axis spray pyrolysis technique. Several characterizations of the $TiO_2$ thin films are covered, such as XRD, UV-Vis spectroscopy, surface profilometry, and I-V analysis.

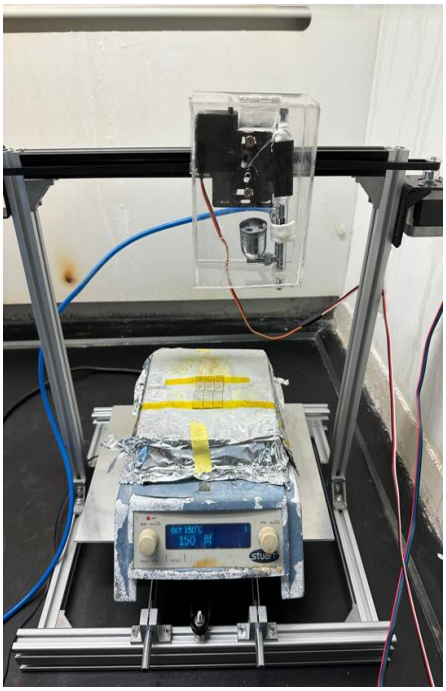

**Figure 1**. The figure 2-Axis Controlled Spray Pyrolysis Deposition Device

### 2.1. Synthesis of $TiO_2$ Nanoparticles

To synthesize $TiO_2$ nanoparticles (NPs), Degussa $TiO_2$ P25 powder, acetic acid, TKC-303 solution, ethanol and Triton X-100 were required. First, 0.3 g P25 powder was mixed with 5.5 ml acetic acid. Then, 20 ml TKC-303 solution was added to the P25 solution and the solution was thoroughly stirred using a magnetic stirrer for a few minutes to ensure complete mixing. Next, 30 ml of ethanol was added to the solution with several drops of Triton X-100. The mixture was then subjected to ultrasonic treatment for 30 minutes to enhance nanoparticle dispersion.

### 2.2. Fabrication of DSSC

Electrodes based on $TiO_2$ nanoparticles were prepared by spray pyrolysis method into various motor speeds which are MS80, MS100, and MS120. With this method, $TiO_2$ NPs were deposited on an opaque FTO substrate in multiple layers to achieve the desired thickness like Figure 2.

This project describes a device i.e., a spray nozzle used in the spray pyrolysis method by incorporating 3D printing. The input of this system by using the push button to control the movement. The control unit is Arduino MEGA and the output is a stepper motor to move the X and Y axis direction and a servo motor to open and close the airbrush as shown in Figure 3.

Figure 4 indicates the hardware setup of the spray-pyrolysis system in the project including essential components such as an air compressor, stepper motor, hot plate, and spray nozzle. This system enables the deposition of metal oxide plates onto a substrate through the atomization of a precursor solution. The precursor solution, containing the necessary chemicals for deposition, is delivered to the spray nozzle and atomized using compressed air. The movement of the spray is precisely controlled by a stepper motor, while the nozzle is set at a fixed height from the substrate. To ensure the desired outcome, the substrate is heated by a hot plate. This heating process helps evaporate the sprayed solution, allowing only the desired particles to be absorbed. The flow rate of the compressed air is regulated by an air compressor regulator, ensuring optimal control over the deposition process. To achieve an even surface on the substrate, the solution is periodically sprayed and given time to evaporate. This careful approach prevents the formation of cracks or uneven surfaces caused by incomplete evaporation, leading to a more uniform and desirable deposition outcome.

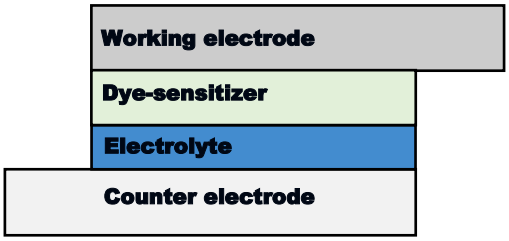


**Figure 2**. The diagram of DSSC fabrication

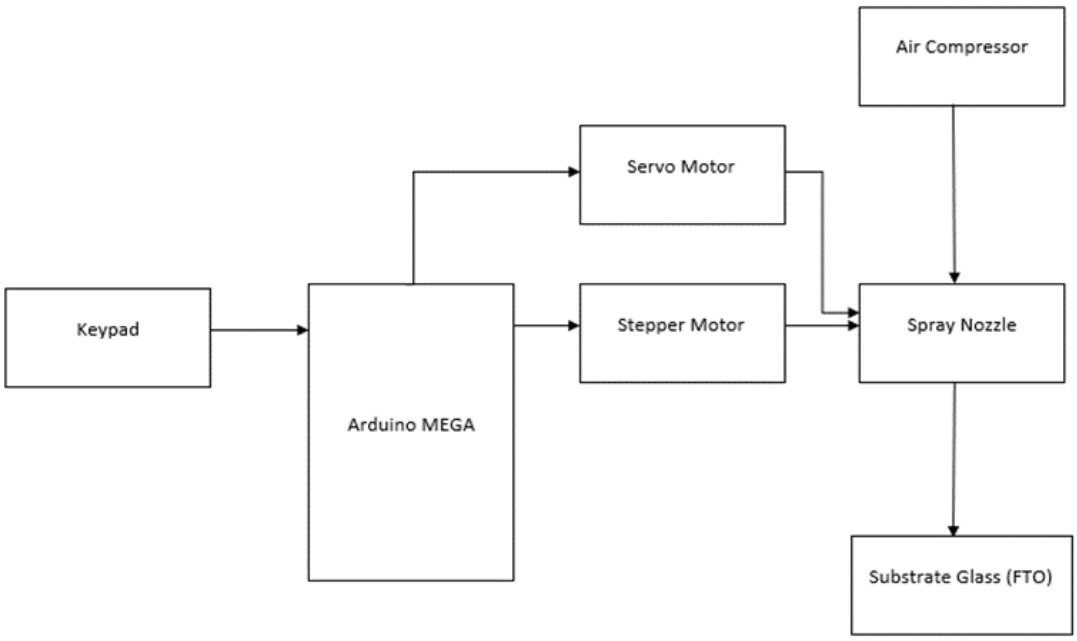


**Figure 3**. The block diagram of the project

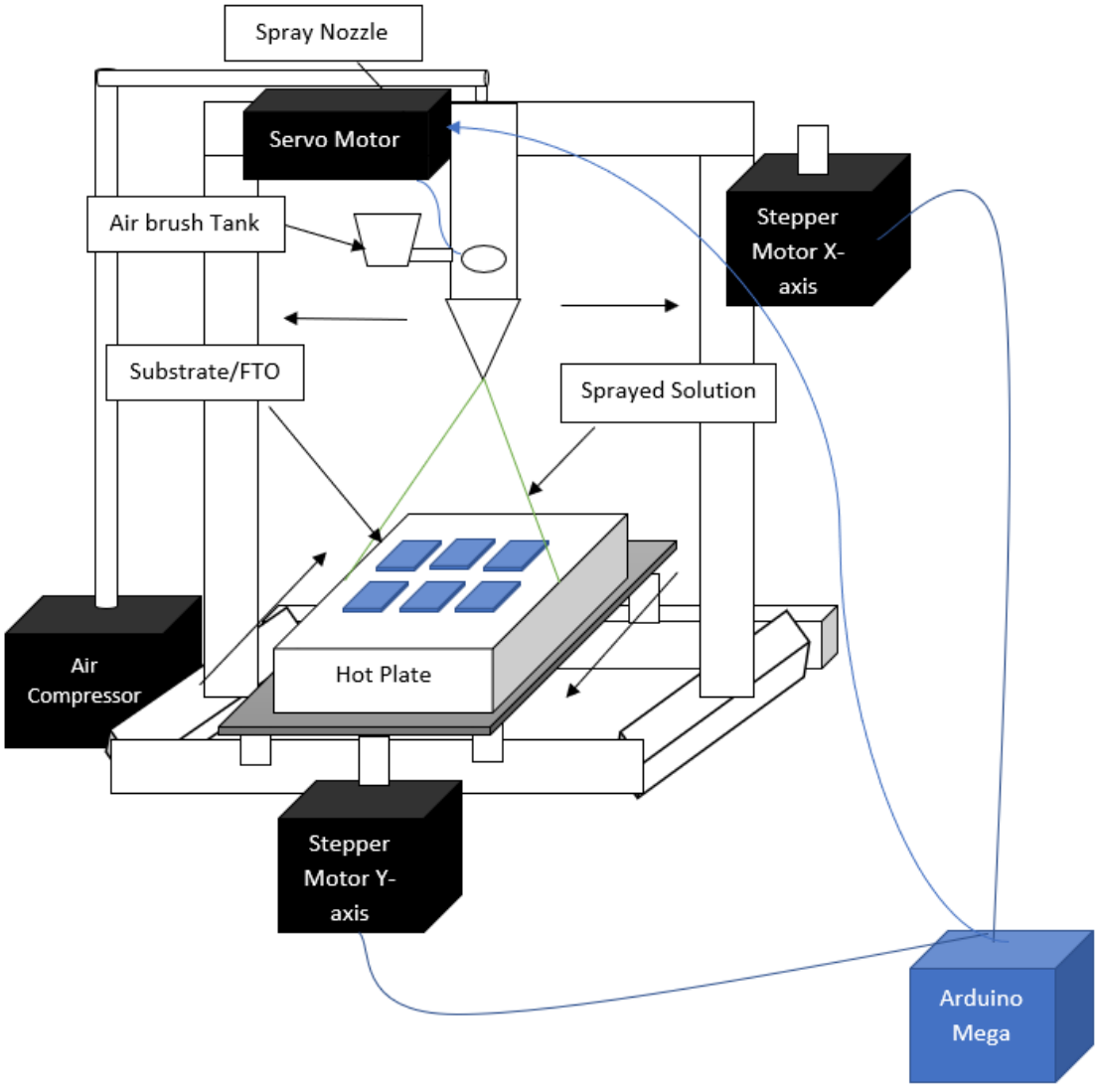


**Figure 4**. The hardware setup

### 2.3. XRD Analysis

The phase purity structure of $TiO_2$ calcined at 450°C was characterized using PANanalytical X-Pert3 Powder X-Ray XRD. The scan axis for 2θ was established with a starting position of 20˚ and an ending position of 80˚. The measurement's scan range was defined in continuous scan mode. The equipment was connected to graphical XRD software (X'PERT HIGHSCORE) which can change and examine the scan of the sample. The scanning sample was operated at tube voltage and current which are 40kV and 40 mA, respectively. The scanning process was done in a small area at room temperature.

### 2.4. UV-Vis Analysis

The UV-Vis spectrometer is an instrument used to measure the absorbance and transmittance of a sample and analyze the optical properties of thin films. To determine the transmittance of light, optical characterizations were carried out and the Lambda 25 UV/VIS spectrophotometer was used to measure the direct band gap energy in the region of 300 nm – 800 nm. Spectroscopic data can be used to determine the band gap of a semiconductor. Equations (1) and (2) below provide the semiconductor band gap computation formulas using Tauc's graphic [25]:

$$\alpha = \frac{1}{t} \times \ln\left(\frac{1}{T}\right) \quad (1)$$

$$(\alpha h\nu)^{1/2} = h\nu - E_g \quad (2)$$

where α represents the absorption coefficient, hv represents the photon energy, A is a constant, and $E_g$ is the bandgap.

### 2.5. Surface Profiler

Measuring surface thickness is done with a profilometer or laser scanner. A smooth surface is one where the Ra is minimal and the deviations are greater.

### 2.6. DSSC Performance

The sun simulator provides a controllable indoor testing environment in a lab setting. A solar simulator will offer an I-V graph displaying the current and voltage produced by the solar cell manufactured under regulated wavelength and energy illumination. The measurement of a solar simulator is fixed during measurement by using Equation (3) that calculate the efficiency of the sample, Equations (4) and (5) focus on the calculation to get the $P_{in}$ and $P_{out}$ value, and Equation (6) to measure the fill factor [26].

$$\eta = \frac{P_{out}}{P_{in}} \times 100\% \quad (3)$$

$$P_{in} = \text{Intensity} \times \text{Effective Surface Area} \quad (4)$$

$$P_{out} = I_{max} \times V_{max} \quad (5)$$

$$FF = \frac{P_{max}}{I_{sc} \times V_{oc}} \quad (6)$$

When plotting an I-V curve for a solar cell, the short-circuit current ($I_{sc}$), open-circuit voltage ($V_{oc}$), current and voltage at maximum power point ($I_{max}$ and $V_{max}$, respectively), and maximum power point ($P_{max}$) are typically highlighted. $I_{max}$ and $V_{max}$ will right away read from the IV measurement data.

The light utilized for the measurement had an intensity of 100 mW/m², or irradiance. An effective solar cell surface area was 0.25 cm². Meanwhile, (FF) was The ratio between the maximum power output ($V_{max} \cdot I_{max}$) and the maximum theoretical output ($V_{oc} \cdot I_{sc}$) that can be used to calculate the efficiency of the device

## 3. RESULTS AND DISCUSSION

### 3.1. XRD Analysis

Figure 5 displays the changes in the XRD pattern of $TiO_2$ nanostructured film fabricated by spray pyrolysis at different motor speeds. According to JCPDS File No. 98-015-4604, $TiO_2$ for samples MS100 is naturally polycrystalline. The (101) diffraction peak has the strongest intensity, while the intensity of other peaks is weak and broad. In the diffraction patterns, distinct peaks for sample MS100 were observed at 2Θ values of 25˚, 37˚, 48˚, 53˚, and 55˚, corresponding to the 101, 004, 200, 105, and 211 planes of $TiO_2$, respectively.

The crystallite size of the film was determined by applying Scherrer's equation at different motor speeds. The crystallite size varied from 16.62 nm to 46.14 nm at MS80. The crystallite size ranged between 30.85 nm and 32.96 nm for MS100. Finally, the crystallite size varied from 16.61 nm to 12.82 nm at MS120.

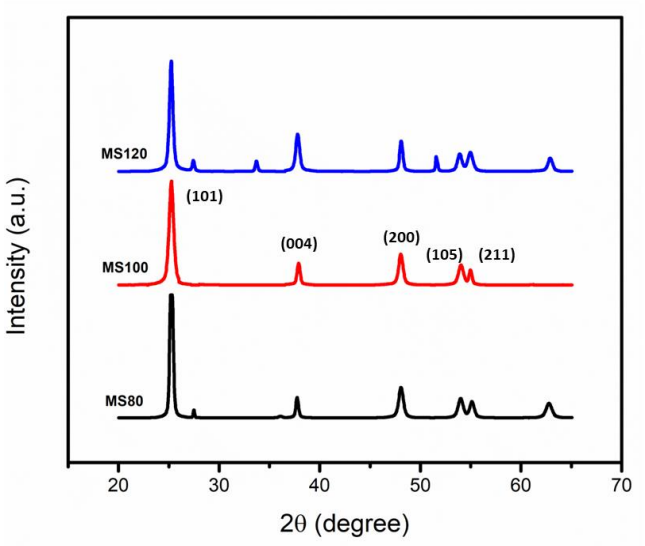


**Figure 5**. The XRD patterns of $TiO_2$ anatase (JCPDS card no. 98-015-4604)

### 3.2. UV-Vis Analysis

The UV–vis spectra of $TiO_2$, samples MS80, MS100, and MS120 are presented in Figure 6. UV-Vis spectra are acquired in this experiment at wavelengths spanning from 300 nm to 800 nm. The absorption edge at approximately 360 nm in $TiO_2$ results from the intrinsic bandgap excitation of anatase, which has a bandgap of 3.2 eV. The increase in motor speed during the $TiO_2$ deposition process results in an effective absorption threshold. As shown in sample MS100, there is a single sharp absorption at around 351 nm in the absorption spectra, which is in good agreement with the bulk anatase's band gap value. This absorption corresponds to 3.2 eV.

According to $TiO_2$ UV-Vis spectroscopy data, the peak absorption occurs between 320 and 360 nm. Figure 6 shows the greatest absorbance at a sample MS120 was found to be at 327 nm, and absorbance fell off sharply after that. The highest absorption at samples MS80 and MS100 was measured at 351 nm. The three observations' absorbance values varied from 0.1 to 1.0 a.u. These differences in peak absorbance wavelengths at various speeds might be related to the $TiO_2$ sample's properties and the testing setup. The $TiO_2$ absorption spectra were examined to evaluate how well it could absorb light in the visible band (300–800 nm). $TiO_2$ typically absorbs light with a peak wavelength of around 320 to 380 nm, indicating its strong absorption of UV radiation within this range.

### 3.3. Surface Profiler Analysis

The surface profiler was used to determine the sample's thickness as shown in Table 1. The $TiO_2$ thickness of measured samples is calculated by using the characteristics of optical films. The thickness for sample MS100 shows the optimum range at 15.17 µm. While excessive thickness for DSSCs encourages aggregation and prevents atom transfer, excessive thinness causes breakage and poor dye absorption. By establishing the right balance, which ensures efficient dye absorption and electron transmission, the DSSC's efficiency is boosted.

### 3.4. DSSC Analysis

Solar cell efficiency is a measure of the performance of DSSC. The energy output produced by a solar cell is divided by the energy input received from sunshine to calculate its efficiency. It displays the solar cell's capacity to transform light into useful electrical energy. The efficiency of a solar cell can be affected by factors such as temperature and light intensity. $TiO_2$-Dye N719 films' I-V graph and efficiency studies demonstrate that annealing them at 450°C increases current and efficiency. The highest efficiency of 9.4% was achieved at sample MS100 as shown in Figure 7. Because it resembles printer action, this speed is thought to be great and suitable for the pressure and spray solution applied to the substrate. MS80 results in a 6.4% efficiency, whereas MS120 results in a somewhat lower 7.8% efficiency.

Under solar illumination, the maximum voltage that can be generated by the cell is equal to the difference between the Fermi level of $TiO_2$ and the redox potential of the electrolyte, around 0.7 V ($V_{oc}$). If there is a light it is connected to it in an "open circuit". Regarding voltage, DSSC has a developed $V_{oc}$ compared to silicon, ranging from 0.7 V to above 0.6 V. Different strategies for using $TiO_2$ in DSSC have been investigated in earlier research.

**Table 1.** The thickness data of $TiO_2$ thin film at various motor speeds

| Motor Speed (steps/rev) | Thickness (µm) |
|---|---|
| MS80 | 13.04 |
| MS100 | 15.17 |
| MS120 | 27.50 |

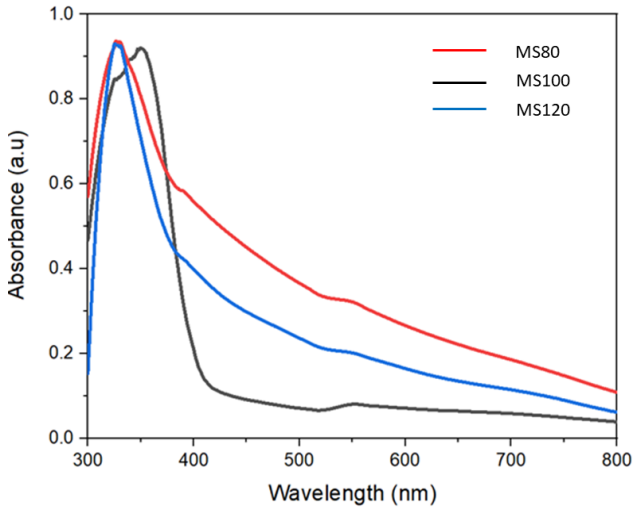


**Figure 6**. The different range of motor speeds for UV-Vis absorption spectra

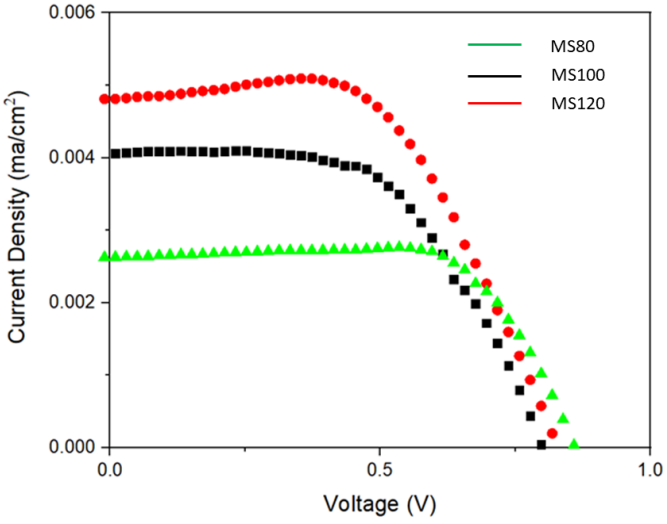


**Figure 7**. The I-V measurement of $TiO_2$ thin film with different motor speeds

## 4. CONCLUSION

The use of the 2-axis Controlled Spray Pyrolysis Deposition Device enabled the effective production of $TiO_2$ thin films at different motor speed deposition rates. The regulated spray speed during deposition resulted in improved performance and consistency of the thin films. After analyzing the XRD, it can be concluded that sample MS100 contains an anatase structure. Meanwhile, the UV-Vis analysis reveals the sample MS100 has a band gap value of 3.2 eV which is the optimum value based on previous studies. The MS100 sample also yields an optimum thickness value of 15.17 μm, which is suitable for DSSC application as determined through surface profiler characterization. The DSSC based on $TiO_2$ nanoparticles was characterized using a current-voltage measurement instrument, achieving a power conversion efficiency of approximately 9.4% for sample MS100. Spray pyrolysis was chosen as the method for producing thin films on a wide scale because of its potential. For DSSCs, it provides a straightforward setup and excellent efficiency.

## ACKNOWLEDGMENTS

The authors also acknowledge the funding that was provided by Universiti Tun Hussein Onn Malaysia (UTHM) through Tier 1 (vot Q369). The author gratefully acknowledges the financial support for this study from the Geran Penyelidikan Pascasiswazah (GPPS), vot H691. Additionally, the authors would like to acknowledge the help of the Faculty of Electrical and Electronic Engineering at Universiti Tun Hussein Onn Malaysia.

## REFERENCES

[1] S. Dixit, "Solar technologies and their implementations: A review," *Materials Today: Proceedings*, vol. 28, pp. 2137–2148, 2020.

[2] K. Sharma, V. Sharma, and S. S. Sharma, "Dye-Sensitized Solar Cells: Fundamentals and Current Status," *Nanoscale Research Letters*, vol. 13, no. 1, p. 381, 2018.

[3] E. Yuliza, S. Saehana, D. Y. Rahman, M. Rosi, K. Khairurrijal, and A. Mikrajuddin, "Enhancement Performance of Dye-Sensitized Solar Cells from Black Rice as Dye and Black Ink as Counter Electrode with Inserting Copper on the Space between TiO2 Particle's by Using Electroplating Method," *Materials Science Forum*, vol. 737, pp. 85–92, 2013.

[4] M. S. Su'ait, M. Y. A. Rahman, and A. Ahmad, "Review on polymer electrolyte in dye-sensitized solar cells (DSSCs)," *Solar Energy*, vol. 115, pp. 452–470, 2015.

[5] E. Maluta, T. Ranwaha, and R. Maphanga, "Density functional theory study of Cyanidin (Cy) dye molecule adsorbed on (100) TiO2 anatase surface for application in DSSCs," in *64th Annual Conference of the South African Institute of Physics*, SA Institute of Physics, 2020, pp. 235–240.

[6] E. Kabir, P. Kumar, S. Kumar, A. A. Adelodun, and K.-H. Kim, "Solar energy: Potential and future prospects," *Renewable and Sustainable Energy Reviews*, vol. 82, pp. 894–900, 2018.

[7] N. Kannan and D. Vakeesan, "Solar energy for future world: - A review," *Renewable and Sustainable Energy Reviews*, vol. 62, pp. 1092–1105, 2016.

[8] S. D. Satpute *et al.*, "Mercurochrome Sensitized ZnO/In2O3 Photoanode for Dye-Sensitized Solar Cell," *ES Energy & Environment*, vol. 9, pp. 89–94, 2020.

[9] C. C.-V. Pablo, R.-R. Enrique, A. R.-G. José, M.-P. Enrique, L.-H. Juan, and N. A.-M. Eddie, "Construction of Dye-sensitized Solar Cells (DSSC) with Natural Pigments," *Materials Today: Proceedings*, vol. 3, no. 2, pp. 194–200, 2016.

[10] N. Narudin, P. Ekanayake, Y. W. Soon, H. Nakajima, and C. M. Lim, "Enhanced properties of low-cost carbon black-graphite counter electrode in DSSC by incorporating binders," *Solar Energy*, vol. 225, pp. 237–244, 2021.

[11] S. N. Abd Majid, A. Q. Ishak, N. A. Nik Ali, M. Z. Daud, and H. Salleh, "The Effect of Ammonium Bromide on Methylcellulose Biopolymer Electrolytes for Electrical Studies," *Solid State Phenomena*, vol. 317, pp. 426–433, 2021.

[12] A. M. S. Nurhaziqah, I. Q. Afiqah, M. F. H. A. Aziz, N. A. N. Aziz, and S. Hasiah, "Optical, Structural and Electrical Studies of Biopolymer Electrolytes Based on Methylcellulose Doped with Ca(NO3)2," *IOP Conference Series: Materials Science and Engineering*, vol. 440, no. 1, p. 12034, 2018.

[13] A. M. S. Nurhaziqah *et al.*, "Optimization of polymer blend electrolytes with tuneable conductivity potentials," *Materials Letters*, vol. 334, p. 133711, 2023.

[14] A. M. S. Nurhaziqah *et al.*, "Microstructure Study of Calcium Manganese Oxide (CaMnO3) as Perovskite Materials," *Journal of Physics: Conference Series*, vol. 1535, no. 1, p. 12024, 2020.

[15] D. G. Saputri *et al.*, "Structural Investigation and Properties Of Tio2 Thin Film Prepared by Sol-Gel Spin Coating," *Indonesian Journal of Applied Physics*, vol. 12, no. 2, p. 251, 2022.

[16] I. Q. Afiqah, N. A. Nik Aziz, A. M. S. Nurhaziqah, S. Hasiah, and M. N. G. Amin, "Marıne calcıum hydroxyapatıte as embryonıc materıal for excellent performance of perovskıte solar cell," *International Journal of Nanoelectronics and Materials*, vol. 13, no. Special Issue ISSTE2019, pp. 107–118, 2020.

[17] A. S. Shikoh, Z. Ahmad, F. Touati, R. A. Shakoor, and S. A. Al-Muhtaseb, "Optimization of ITO glass/TiO2 based DSSC photo-anodes through electrophoretic deposition and sintering techniques," *Ceramics International*, vol. 43, no. 13, pp. 10540–10545, 2017.

[18] S. Bera, D. Sengupta, S. Roy, and K. Mukherjee, "Research into dye-sensitized solar cells: a review highlighting progress in India," *Journal of Physics: Energy*, vol. 3, no. 3, p. 032013, 2021.

[19] A. Agrawal, S. A. Siddiqui, A. Soni, K. Khandelwal, and G. D. Sharma, "Performance analysis of TiO2 based dye sensitized solar cell prepared by screen printing and doctor blade deposition techniques," *Solar Energy*, vol. 226, pp. 9–19, 2021.

[20] A. S. AlShammari, M. M. Halim, F. K. Yam, and N. H. M.

Kaus, "Synthesis of Titanium Dioxide (TiO2)/Reduced Graphene Oxide (rGO) thin film composite by spray pyrolysis technique and its physical properties," *Materials Science in Semiconductor Processing*, vol. 116, p. 105140, 2020.

[21] E. Moustafa, J. G. Sánchez, L. F. Marsal, and J. Pallarès, "Stability Enhancement of High-Performance Inverted Polymer Solar Cells Using ZnO Electron Interfacial Layer Deposited by Intermittent Spray Pyrolysis Approach," *ACS Applied Energy Materials*, vol. 4, no. 4, pp. 4099–4111, 2021.

[22] A. Aboulouard *et al.*, "Dye sensitized solar cells based on titanium dioxide nanoparticles synthesized by flame spray pyrolysis and hydrothermal sol-gel methods: A comparative study on photovoltaic performances," *Journal of Materials Research and Technology*, vol. 9, no. 2, pp. 1569–1577, 2020.

[23] O. Malik, F. J. D. La Hidalga-Wade, and R. R. Amador, "Spray Pyrolysis Processing for Optoelectronic Applications," in *Pyrolysis*, M. Samer, Ed., Rijeka: InTech, 2017, p. Ch. 8.

[24] F. A. Unal, S. Ok, M. Unal, S. Topal, K. Cellat, and F. Şen, "Synthesis, characterization, and application of transition metals (Ni, Zr, and Fe) doped TiO2 photoelectrodes for dye-sensitized solar cells," *Journal of Molecular Liquids*, vol. 299, p. 112177, 2020.

[25] T. Siddaiah, P. Ojha, N. O. Gopal, C. Ramu, and H. Nagabhushana, "Thermal, structural, optical and electrical properties of PVA/MAA:EA polymer blend filled with different concentrations of Lithium Perchlorate," *Journal of Science: Advanced Materials and Devices*, vol. 3, no. 4, pp. 456–463, 2018.

[26] N. Kutlu, "Investigation of electrical values of low-efficiency dye-sensitized solar cells (DSSCs)," *Energy*, vol. 199, p. 117222, 2020.